



المجلة العلمية لجامعة الملك فيصل The Scientific Journal of King Faisal University

العلوم الأساسية والتطبيقية
Basic and Applied Sciences



Minimising the Heat Affected Zone in the Laser Cutting of Ti-6Al-4V Sheets using the Monte Carlo Method

Ekhlas Jabir Mahmood

Department of Physics, College of Education for Girls, University of Kufa, Kufa, Iraq

تقليل المنطقة المتأثرة بالحرارة في القطع بالليزر لألواح Ti-6Al-4V باستعمال طريقة مونت كارلو

اخلاص جابر محمود

قسم الفيزياء، كلية التربية للبنات، جامعة الكوفة، الكوفة، العراق

KEYWORDS

الكلمات المفتاحية

CO₂ laser, artificial neural network (ANN), cutting speed, beam power, assist gas pressure
ليزر CO₂، شبكة الذكاء الاصطناعي، سرعة القطع، طاقة الشعاع، ضغط الغاز المساعد

RECEIVED

الاستقبال

15/09/2020

ACCEPTED

القبول

01/11/2020

PUBLISHED

النشر

01/06/2021



<https://doi.org/10.37575/sj.0029>

ABSTRACT

This research attempts to minimise the heat affected zone (HAZ) width that forms in the laser cutting process of Ti-6Al-4V sheets. The experimental results of the HAZ for 32 sets of five CO₂ laser cutting parameters (with the assist pressure of argon gas) were used to build the artificial neural network (ANN) model, each with a different material thickness, cutting speed, laser beam power, assist gas pressure and lens focal length percentage. A relationship formula was derived by connecting the laser cutting parameters based on the connection weights obtained from the developed ANN model. The MAPE value for the comparison between the predicted and experimental HAZ width was 4.192%. The Monte Carlo optimisation method was performed using 2,000 simulations to identify a suitable optimal solution. The results showed that the most effective transfer function type in the hidden layers was the linear function. The model was highly sensitive for the cutting speed (CS), assist gas pressure (GP) and beam power (BP) parameters and less sensitive for the parameters of thickness (T) and lens focal length (LFL). The optimum values of the laser cutting parameters that produced a minimum value of HAZ was T = 1 mm, LFL = 30%, BP = 3 kW, CS = 1 m/min and GP = 14 bars.

المخلص

يقدم هذا البحث محاولة لتقليل عرض (مساحة) المنطقة المتأثرة بالحرارة والتي تكونت بسبب عمليات القطع بالليزر لألواح Ti-6Al-4V. تم استعمال نتائج تجريبية لمنطقة متأثرة بالحرارة (HAZ) لـ 32 مجموعة من خمسة معاملات قطع ليزر CO₂ (باستخدام الضغط المساعد لغاز الأرجون)، وهي: سمك المادة، وسرعة القطع، وطاقة شعاع الليزر، وضغط الغاز المساعد ونسبة البعد البؤري للعدسة، لبناء نموذج الذكاء الاصطناعي (ANN). تم اشتقاق صيغة العلاقة من خلال ربط معاملات القطع بالليزر بناءً على أوزان الارتباط التي تم الحصول عليها من نموذج ANN المطور. بلغت قيمة MAPE للمقارنة (للموازنة) بين عرض (HAZ) المتوقع والتجريبي (4.192%). وتم تنفيذ طريقة الأمثلية مونت كارلو باستخدام 2000 نموذج محاكاة لتحديد الحل الأمثل المناسب. أظهرت النتائج أن أفضل نوع فعال من دوال التحويل في الطبقات المخفية هي الدالة الخطية. وكان النموذج حساساً للغاية لمعاملات سرعة القطع (CS)، وضغط الغاز المساعد (GP)، وطاقة الشعاع (BP)، وأقل حساسية لمعاملات السمك (T)، والبعد البؤري للعدسة (LFL). كانت القيم المثلى لمعاملات القطع بالليزر التي تنتج أقل قيمة لـ (HAZ) هي السمك (T = 1 mm)، والبعد البؤري للعدسة (LFL = 30%)، وطاقة شعاع (BP = 3 kW)، وسرعة القطع (CS = 1 م / دقيقة)، وضغط الغاز المساعد (GP = 14 بار).

1. Introduction

Specialists have developed many techniques for processing different forms, sizes and shapes of materials (complex and simple) in order to keep pace with the current progress of advanced manufacturing processes as well as taking environmental protection into account and minimising time, effort and cost (Ghany and Newishy, 2005). The use of lasers in cutting processes is among the best of these technologies, as this technology meets many of the goals of advanced industries. This approach is summarised by concentrating the laser beam on the surface of the workpiece in order to melt or evaporate the material at an elevated temperature. This technology has allowed very small workpieces to be cut within a micro range and has produced products free of mechanical pressure distortions compared to other technologies (Yusoff et al., 2008). As a result of the high temperature, which is generated by the focus of the laser beam on the surface of the material, the areas surrounding the cutting region are affected and unwanted phenomena occur, such as a decline in weldability, surface cracking, deformation, embrittlement and fatigue resistance. This area of the material, which has a microstructure and mechanical features and is influenced by the heat generated during the laser cutting process, is called the heat affected zone (HAZ). The quality of the laser cutting process depends on the physical properties of the material. These properties can be limited by heat conduction, plasma development, phase change, molten-layer flow and surface absorption (Ghany and Newishy, 2005). Determining the relationship between cutting conditions and the HAZ as well as choosing appropriate laser cutting parameters is very important for minimising the HAZ. A number of studies have been carried out to investigate the effect of the laser cutting parameters on the efficiency of the cutting process and the HAZ, such as Sheng and Joshi (1995), Hamoudi (1997), Nagarajan

(2000), Quintero et al. (2004), Shiue et al. (2004), Almeida et al. (2006), Davim et al. (2008), Dubey and Yadava (2008), Radovanovic and Madic (2011), Eltawahni et al. (2011), Lee and Te Chen (2011), Pandey and Dubey (2012), Miraoui et al. (2013) and Miraoui et al. (2014). Most of these studies showed that the HAZ increases with increasing laser power and decreases with increasing cutting speed. Recently, an artificial neural network (ANN) technique has been used widely to develop a complex relationship between the input and output parameters. The ANN can be considered a very good generalisation efficiency method (Topçu et al., 2009). Many researchers have used the ANN technique in order to predict the parameters of the laser cutting process, such as Liao and Chen (1994), Sarkar et al. (2006), Dhara et al. (2008), Biswas et al. (2010), Kamrunnihar and Macdonald (2011) and Madić and Radovanović (2012). These studies concluded that the use of the ANN offers an alternative computing paradigm that is closer to reality and that has the ability to develop an accurate relationship to predict parameters. The Monte Carlo optimisation procedure can be considered as an appropriate simple and efficient procedure to determine the optimum values of laser cutting parameters.

From the above, in the process of predicting the characteristics of the HAZ, such as width and depth, researchers have used many different methods and approaches within their studies, but most have required a model to be developed and new data entered, and this process naturally requires time and expertise. With an accessible equation for ease while preserving the same accuracy of outcomes, the process of merging artificial intelligence and optimisation techniques has been developed. In this study, 32 sets of five CO₂ laser cutting parameters (1 mm beam diameter, continuous wave, 10.64 μm wavelength, beam mode as Gaussian distribution (TEM₀₀), with the assist pressure of argon gas) were used to build the ANN model, each with a different

material thickness, cutting speed, laser beam power, assist gas pressure and lens focal length percentage. The Monte Carlo procedure was implemented to achieve the values of optimal laser cutting parameters that minimise the HAZ width for a Ti-6Al-4V alloy, depending on the results of the ANN modelling.

2. Material and Methods

2.1. Experimental Data:

To build the ANN model, 32 sets of five CO₂ laser cutting parameters were used. The experiment runs were conducted with argon as the assist gas, and the pressure of argon gas ranged between 10 bars and 14 bars (Table 1). A Ti-6Al-4V alloy, which is frequently used in the aerospace industry, was used in this study with two thicknesses, 1.0 mm and 6.35 mm.

Table 1. Experimental data details.

No.	HAZ (µm)	Thickness (mm)	Lens focal length %	Beam power (kW)	Cutting speed (m/min)	Gas pressure (bar)
1	423	1	30	3	0.5	10
2	423	6.35	30	3	0.5	10
3	430	1	80	3	0.5	10
4	423	6.35	80	3	0.5	10
5	486	1	30	4	0.5	10
6	474	6.35	30	4	0.5	10
7	448	1	80	4	0.5	10
8	460	6.35	80	4	0.5	10
9	347	1	30	3	1	10
10	355	6.35	30	3	1	10
11	340	1	80	3	1	10
12	370	6.35	80	3	1	10
13	393	1	30	4	1	10
14	380	6.35	30	4	1	10
15	378	1	80	4	1	10
16	385	6.35	80	4	1	10
17	422	1	30	3	0.5	14
18	420	6.35	30	3	0.5	14
19	387	1	80	3	0.5	14
20	437	6.35	80	3	0.5	14
21	395	1	30	4	0.5	14
22	401	6.35	30	4	0.5	14
23	381	1	80	4	0.5	14
24	462	6.35	80	4	0.5	14
25	301	1	30	3	1	14
26	358	6.35	30	3	1	14
27	308	1	80	3	1	14
28	367	6.35	80	3	1	14
29	380	1	30	4	1	14
30	340	6.35	30	4	1	14
31	377	1	80	4	1	14
32	366	6.35	80	4	1	14
Max.	486	6.35	80	4	1	14
Min.	301	1	30	3	0.5	10

2.2. Artificial Neural Network Technique:

The idea of developing the ANN was inspired by mimicking the biological neural system. Today, this technique is independent of pre-established basics or models and has become an alternative computing pattern that is closer to reality (Akbari et al., 2016). In order to understand the mechanisms behind the ANN it is necessary to get familiar with its components. The ANN consists of elemental processors, known as neurons, that perform simple and specific tasks. These neurons handle the information it receives by implementing a mathematical activation function as its net input. The output is produced as a signal. A neuron's net input is principally a weighted sum of all its inputs. Each neuron is connected with others through links. The task of these links is to transmit the signals between the neurons. Each connection link has a related weight (W_{ij}) that is used to adjust the signals transmitted. The structure of the ANN is divided into layers, usually three, each one involving a group of slabs and each slab involving a group of neurons. The three layers of the ANN are called the input, hidden and output layer. The main task of the input layer is to receive information (a set of parameters representing the conditions of the problem) and transmit it to the hidden layer. Each neuron found in the input layer is interconnected with all the neurons in the hidden layer. The main task of a hidden layer is to analyse and process information. This layer generates a suitable internal representation by carrying out a pattern appreciation from all the received information and re-coding it so that the essential properties of the patterns are

preserved. In the same way, each neuron within the hidden layer is interconnected with all the neurons of the output layer. The main task of the output layer is to receive this analysis and translate it into a meaningful interpretation to interconnect it back to the environment.

Generally, the activation function is divided into four styles: probabilistic, linear, binary and sigmoid. The most common styles are

- Linear function: $f(x) = m + bx$ (1)
- Logistic sigmoid function: $f(x) = \frac{1}{1+e^{-\sigma x}}$ (2)

Due to the variety of problems, ANN models are divided into many types. For this study, we are going to focus on the algorithm of the feed-forward back propagation ANN type, which is used for prediction problems. In an ANN, specific mapping is implemented through the learning or training process by iteratively adjusting the weights, testing the process to determine the lowest error and a validation process to display the outputs of prediction, momentum and the learning rate to control the stability and speed of the training progression (Feng et al., 2006). A PC-based commercial software system called Neuframe Version 4.0 (Neuscience 2000) was used, in which the optimal network architecture was determined by trial and error.

2.3. The Monte Carlo Technique:

The Monte Carlo algorithm can be considered as a simple and efficient mathematical optimisation technique used for solving a broad variety of problems. The procedure is to use the randbetween function in order to produce a uniform generation of random numbers (r_i, j) distributed in a range (maximum, minimum) within a short computation time (Kroese et al., 2014). To calculate the optimum width of the HAZ, the randomised values were generated for each of the laser cutting parameters, and then the mathematical function based on the ANN was used to calculate the HAZ value. After completing the calculations, the optimum values of laser cutting parameters that met a minimum value of HAZ were determined.

2.4. Statistical Criteria:

In order to evaluate the accuracy of the results of the ANN model, a comparison between the experimental and predicted results was conducted by using the statistical criteria, such as the coefficient of determination (R^2), the root mean square error (RMSE), the mean error (ME) and the mean absolute error (MAE):

$$R^2 = \frac{[\sum(x-\bar{x})-(y-\bar{y})]^2}{[\sum(x-\bar{x})^2-(y-\bar{y})^2]} \quad (3)$$

$$RMSE = \sqrt{\frac{1}{n} \sum_{i=1}^n (R_s - R_0)^2} \quad (4)$$

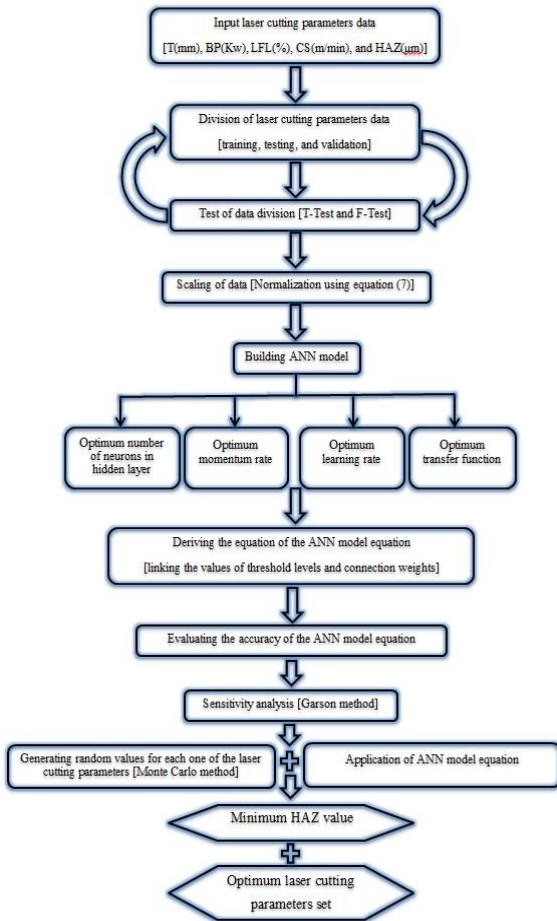
$$ME = \frac{1}{n} \sum_{i=1}^n (R_s - R_0) \quad (5)$$

$$MAE = \frac{\sum_{i=1}^n |(R_s - R_0)|}{n} \quad (6)$$

3. Methodology

The procedure used to pick the optimum laser cutting parameters leading to the minimisation of the HAZ is illustrated in the flow chart below (Figure 1).

Figure 1. Flowchart of the procedure



3.1. Division of Data:

The 32 datasets of laser cutting parameters were divided into two sets randomly (learning and validation). In general, 80% of the total data was used for learning and 20% was used for validation. The learning dataset was divided into 30% for the testing set and 70% for the training set. The distribution of data for each dataset was determined to be statistically consistent and, thus, represent the convergent statistical population.

3.2. Tests for Divisions:

To examine the normal distribution of dataset divisions and assess whether the means of these compared groups for training, testing and validation were statistically different from each other, a T-test and F-test were carried out (Trochim and Donnelly, 2001). The tests showed that the dataset divisions met the normal distribution requirements (Table 2).

Table 2. T-test and F-test results for the ANN input and output parameters

Data Set	Mean	Variance	-Value	-Critical Situation	F-Value	-Critical Situation
Gas Pressure (bar)						
Testing	12.00	4.57	0.59	2.18	Accept	1.07
Validation	11.33	4.27			4.88	Accept
Thickness (mm)						
Testing	3.01	7.67	-0.44	2.18	Accept	0.89
Validation	3.68	8.39			0.25	Accept
Lens Focal Length (%)						
Testing	61.25	669.64	0.44	2.18	Accept	0.89
Validation	55.00	750.00			0.25	Reject
Beam Power (kW)						
Testing	3.63	0.27	0.44	2.18	Accept	0.89
Validation	3.50	0.30			0.25	Reject
Cutting Speed (m/min)						
Testing	0.75	0.07	-0.59	2.18	Accept	1.07
Validation	0.83	0.07			4.88	Accept
Haz (°M) Argon						
Testing	395.3	1287.98	0.61	2.18	Accept	0.44
Validation	380.6	2943.07			0.25	Reject

3.3. Scaling of the Data:

In order to ensure that all the parameters of the laser cutting process received the same attention during each stage of learning, a simple scaling was conducted by using the maximum and minimum for each parameter, as in equation 7. The scaling process eliminates parameter values by arranging them between 0 and 1.

$$X_n = \frac{X - X_{min}}{X_{max} - X_{min}} \quad (7)$$

3.4. Artificial Neural Network Model Setup:

The presence of the many variables (input and output parameters) makes the task of building the ANN model more difficult, therefore, determining the optimum parameters was based on trial and error. First, the outline of the architecture of the ANN model was three layers – the input, hidden and output layer. According to previous studies, the hidden layer can approximate to any continuous function (Cybenko, 1992; Hornik et al., 1989). The input layer includes five neurons, one neuron in each of the input laser cutting parameters (thickness (T), lens focal length (LFL), beam power (BP), cutting speed (CS) and assist gas pressure (GP)). The output layer includes one neuron for each output parameter (HAZ). There are three neurons in the hidden layer, which was determined according to the minimum (RMSE), ME and maximum (R) (Table 3 and Figure 2). It was also found that the ANN model gives the best prediction for data when the momentum rate and learning rate are equal to 0.7 and 1.6, respectively (Figures 3 and 4). The number of iterations was 50,000 because there was no further progress in the performance of the ANN model after this number. In the same way, the selection of the type of transfer function was based on the performance of the ANN model, the optimum prediction achieved using the sigmoid, linear and tangent transfer functions for the input, hidden and output layers, respectively (Table 4).

Table 3. Performance of the ANN model with different hidden layer neurons (learning rate = 1.6 and momentum rate = 0.7)

No. of Hidden Layer Neurons	RMSE	MAE	R
1	13.453	9.712	0.984
2	9.897	6.603	0.985
3	8.225	6.440	0.987
4	9.346	8.193	0.988
5	8.364	6.942	0.988
6	8.614	7.351	0.988
7	8.835	7.638	0.988
8	9.027	7.860	0.988
9	9.196	8.041	0.988
10	9.346	8.193	0.988

Figure 2. Structure of the ANN model

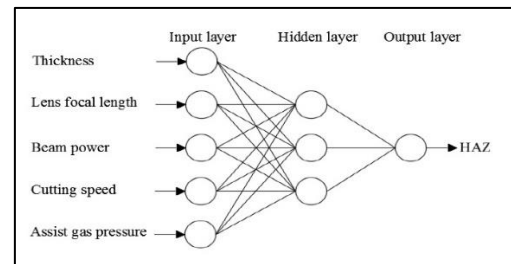


Figure 3. Performance of the ANN model with different momentum rates (learning rate = 1.6 and hidden layer neurons = 3).

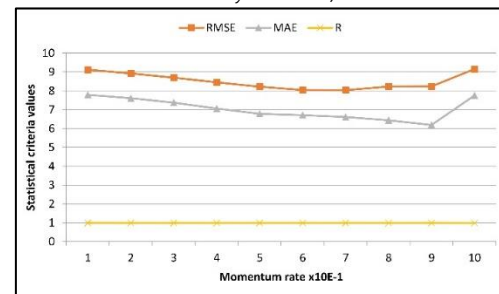


Figure 4. Performance of the ANN model with different learning rates (momentum rate = 0.7 and hidden layer neurons = 3).

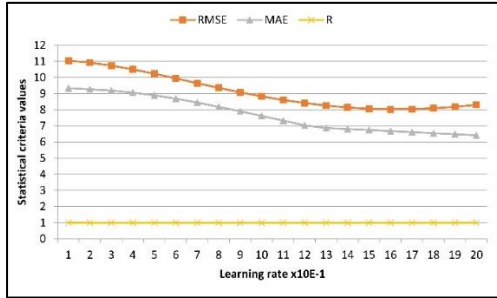


Table 4. Performance of the ANN model with different transfer function types (momentum rate = 0.7, learning rate = 1.6 and hidden layer neurons = 3).

Trial No.	Input layer	Hidden layer	Output layer	RMSE	ME	R
1	S	S	S	30.441	22.597	0.931
2	S	S	L	83.269	52.479	0.879
3	S	S	T	29.856	25.069	0.889
4	S	L	S	8.028	6.679	0.987
5	S	L	L	US	US	US
6	S	L	T	US	US	US
7	S	T	S	37.519	28.312	0.823
8	S	T	L	30.516	28.106	0.984
9	S	T	T	27.277	22.132	0.839
10	L	S	S	37.936	33.336	0.926
11	L	S	L	19.639	14.129	0.961
12	L	S	T	74.869	63.101	0.764
13	L	L	S	8.402	7.074	0.987
14	L	L	L	US	US	US
15	L	L	T	137.674	128.458	-0.641
16	L	T	S	41.657	32.187	0.874
17	L	T	L	US	US	US
18	L	T	T	32.771	26.286	0.774
19	T	S	S	43.070	34.547	0.878
20	T	S	L	32.047	27.901	0.924
21	T	S	T	42.507	33.384	0.945
22	T	L	S	8.334	6.967	0.987
23	T	L	L	US	US	US
24	T	L	T	17.832	13.179	0.970
25	T	T	S	42.651	32.911	0.875
26	T	T	L	74.871	67.704	0.987
27	T	T	T	49.502	35.397	0.624

S: Sigmoid, L: Linear, T: Tangent, US: Un Stable Solution

4. Results and Discussion

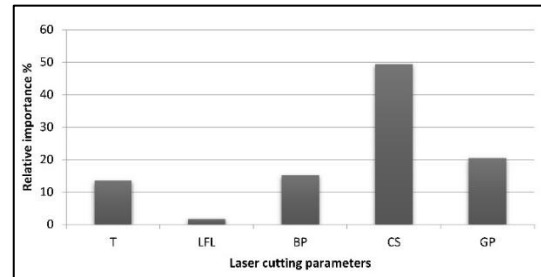
The outcomes of the T-test and F-test refer to the credibility of the relationship between these groups from a statistical point of view. As can be seen in Table 3, there is a significant decrease in the RMSE and MAE when using three neurons instead of single neurons. Figure 3 refers to the inflection point of the RMSE curve at a momentum rate of 0.7, while the minimum MAE value met at a point of momentum rate of 0.9. Figure 4 refers to the parallel decrease of the RMSE and MAE values until the point of learning rate of 1.6. After this point a reasonable increase in the RMSE can be seen and also in the MAE. It is evident from the statistical criteria values included in Table 4 that the sigmoid-learning-sigmoid functions category for the input-hidden-output layers, respectively, gave excellent prediction results. The value of the correlation coefficient remained approximately constant in all cases and its value ranged from 98.7% to 98.9%. The results for running the ANN model indicate the high prediction accuracy of the HAZ-width values within the scope of the laser cutting parameters. The results and the accuracy of the ANN prediction are consistent with the accuracy and results of the previous studies by Madić and Radovanović (2012) and Desai and Shaikh (2012). When a comparison was conducted between their models, the ANN model was the better in performance. Also, the final results indicate the importance of having a good distribution of input and output laser cutting parameter groups (training, testing and validation).

4.1. Sensitivity Analysis:

The laser cutting parameters differ from each other in the amplitude of the effect on the cutting process. In order to identify which of these parameters has the most significant impact, a sensitivity analysis was carried out using the Garson (1991) method based on

the connection network weights of the ANN model. The results illustrated that the cutting speed (CS), assist gas pressure (GP) and beam power (BP) parameters had the most weighty effect on the predicted HAZ with a relative importance of 49.35%, 20.39% and 15.14%, respectively, while the parameters for thickness (T) and lens focal length (LFL) had a relative importance of 13.42% and 1.69%, respectively (Figure 5).

Figure 5. Sensitivity analysis results for the laser cutting parameters.



4.2. Artificial Neural Network Model Equation:

In order to derive a relationship formula to link the laser cutting parameters, the distribution of the values of the threshold levels and connection weights for the laser cutting parameters, obtained from the final ANN model, were used. The predicted HAZ can be expressed as a linear function, as in equation 8:

$$HAZ (mm) = 0.479 + 0.0026 T (mm) + 0.0026 LFL (\%) + 0.024BP (kW) - 0.0084 CS \left(\frac{mm}{sec}\right) - 0.0064 GP (bar) \quad (8)$$

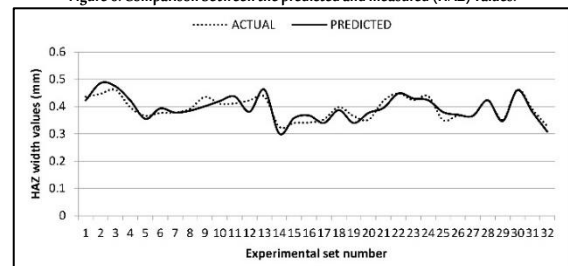
To evaluate the accuracy of the ANN model equation, the mean absolute percentage error (MAPE) criteria was calculated according to equation 9. This criteria states that the accuracy of the ANN model equation can be considered accepted if the MAPE value is less than 30%.

$$MAPE = \frac{1}{N} \sum_{i=1}^N \left| \frac{A_i - P_i}{A_i} \right| \times 100\% \quad (9)$$

where A_i and P_i represent the actual and the predicted values, respectively.

To calculate the MAPE value, an equation was employed based on all the laser cutting parameter groups (training, testing and validating) as the measured data and the ANN model results as the predicted data. The result of the MAPE value for these calculations was 4.192%, and this percentage was considered to be acceptable. To explain the capability of the ANN model equation, the predicted values of the HAZ were plotted against the measured HAZ values, as seen in Figure 6. It can be seen that the predicted HAZ results of the ANN model equation demonstrated a good agreement with the actual measurements.

Figure 6. Comparison between the predicted and measured (HAZ) values.



4.3. Monte Carlo Optimisation:

The randomised values were generated for each of the laser cutting parameters, then the HAZ values were calculated using equation 8. In order to identify the acceptable optimal solution, Monte Carlo

algorithms were performed using 2,000 simulations. The results were in line with the experimental results and proved that the minimum value of the HAZ width could be accomplished using a workpiece with $T = 1$ mm, $LFL = 30\%$, $BP = 3$ kW, $CS = 1$ m/min and $GP = 14$ bars.

5. Conclusions

This work involves an analysis of 32 sets of five CO₂ laser cutting parameters (with the assist pressure of argon gas) used to build an ANN model, each with a different material thickness, cutting speed, laser beam power, assist gas pressure and lens focal length percentage. A linear relationship formula was derived by linking the laser cutting parameters based on the connection weights obtained from the developed ANN model, and this equation gave an acceptable MAPE value. Monte Carlo algorithms were performed using 2,000 simulations to identify the acceptable optimal solution. The conclusions are summarised in the following points:

- The linear function was the best form of effective transfer function in the hidden layers.
- The relationship between the width of the HAZ and the most laser cutting parameters was close to linear.
- The model was highly sensitive for cutting speed (CS), assist gas pressure (GP) and beam power (BP) parameters and less sensitive for the parameters of thickness (T) and lens focal length (LFL).
- The minimum value of the HAZ can be obtained with $T = 1$ mm, $LFL = 30\%$, $BP = 3$ kW, $CS = 16.6667$ mm/sec and $GP = 14$ bars.

Biography

Ekhlal Jabir Mahmood

Lecturer at the Department of Physics, College of Education for Girls, University of Kufa, Kufa, Iraq, 009647811185206, ikhlal.alleebawi@uokufa.edu.iq

Miss Mahmood graduated from the University of Kufa and received a master's degree from the same University in 2013 in laser physics. She is a member of the Quality and Academic Accreditation Committee and is a researcher interested in laser applications and simulating laser processes. She has had seven research articles published in national and Scopus-indexed international journals and participated in three scientific conferences. ORCID: <https://orcid.org/0000-0001-5963-492X>. Website: <http://staff.uokufa.edu.iq/?ikhlal.alleebawi>.

References

- Akbari, M., Saedodin, S., Panjehpour, A., Hassani, M., Afrand, M. and Torkamany, M. J. (2016). Numerical simulation and designing artificial neural network for estimating melt pool geometry and temperature distribution in laser welding of Ti6Al4V alloy. *Optik*, **127**(23), 11161–72.
- Almeida, I. A., De Rossi, W., Lima, M. S. F., Berretta, J. R., Nogueira, G. E. C., Wetter, N. U. and Vieira Jr, N. D. (2006). Optimization of titanium cutting by factorial analysis of the pulsed Nd: YAG laser parameters. *Journal of Materials Processing Technology*, **179**(1–3), 105–10.
- Biswas, R., Kuar, A. S., Biswas, S. K. and Mitra, S. (2010). Artificial neural network modelling of Nd: YAG laser microdrilling on titanium nitride–alumina composite. *Proceedings of the Institution of Mechanical Engineers, Part B: Journal of Engineering Manufacture*, **224**(3), 473–82.
- Desai, C. K. and Shaikh, A. (2012). Prediction of depth of cut for single-pass laser micro-milling process using semi-analytical, ANN and GP approaches. *The International Journal of Advanced Manufacturing Technology*, **60**(9–12), 865–82.
- Cybenko, G. (1992). Approximation by superpositions of a sigmoidal function. *Mathematics of Control, Signals and Systems*, **5**(4), 455.
- Dahotre, N. B. and Harimkar, S. P. (2008). *Laser Fabrication and Machining of Materials*, Springer: Berlin.
- Davim, J. P., Barricas, N., Conceicao, M. and Oliveira, C. (2008). Some experimental studies on CO₂ laser cutting quality of polymeric materials. *Journal of Materials Processing Technology*, **198**(1–3), 99–104.
- Dhara, S. K., Kuar, A. S. and Mitra, S. (2008). An artificial neural network approach on parametric optimization of laser micro-machining of die-steel. *The International Journal of Advanced Manufacturing Technology*, **39**(1–2), 39–46.
- Dubey, A. K. and Yadava, V. (2008). Multi-objective optimisation of laser beam cutting process. *Optics and Laser Technology*, **40**(3), 562–70.
- Eltawahni, H. A., Olabi, A. G. and Benyounis, K. Y. (2011). Investigating the CO₂ laser cutting parameters of MDF wood composite material. *Optics and Laser Technology*, **43**(3), 648–59.
- Feng, C. X. J., Yu, Z. G. and Kusiak, A. (2006). Selection and validation of predictive regression and neural network models based on designed experiments. *IIE Transactions*, **38**(1), 13–23.
- Garson, D. G. (1991). Interpreting neural network connection weights. *AI Expert*, **6**(4), 47–51.
- Ghany, K. A. and Newishy, M. (2005). Cutting of 1.2 mm thick austenitic stainless steel sheet using pulsed and CW Nd: YAG laser. *Journal of Materials Processing Technology*, **168**(3), 438–47.
- Hamoudi, W. K. (1997). The effects of speed and processing gas on laser cutting of steel using a 2 kW CO sub 2 laser. *International Journal for the Joining of Materials (Denmark)*, **9**(1), 31–6.
- Hornik, K., Stinchcombe, M. and White, H. (1989). Multilayer feedforward networks are universal approximators. *Neural Networks*, **2**(5), 359–66.
- Kamrunnahar, M. and Urquidi-Macdonald, M. (2011). Prediction of corrosion behaviour of Alloy 22 using neural network as a data mining tool. *Corrosion Science*, **53**(3), 961–7.
- Kroese, D. P., Brereton, T., Taimre, T. and Botev, Z. I. (2014). Why the Monte Carlo method is so important today. *Wiley Interdisciplinary Reviews: Computational Statistics*, **6**(6), 386–92.
- Lee, H. T. and Te Chen, C. (2011). Numerical and experimental investigation into effect of temperature field on sensitization of AISI 304 in butt welds fabricated by gas tungsten arc welding. *Materials Transactions*, **52**(7), 1506–14.
- Liao, T. W. and Chen, L. J. (1994). A neural network approach for grinding processes: modelling and optimization. *International Journal of Machine Tools and Manufacture*, **34**(7), 919–37.
- Madić, M. J. and Radovanović, M. R. (2012). Analysis of the heat affected zone in CO₂ laser cutting of stainless steel. *Thermal Science*, **16**(suppl. 2), 363–73.
- Mahmood, A. J. (2018). Theoretical study of comparative between the speed of penetration and cutting using a laser beam. *Engineering and Technology Journal*, **36**(Part B Scientific), 37–43.
- Miraoui, I., Boujelbene, M. and Bayraktar, E. (2013). Effects of laser cutting main parameters on microhardness and microstructure changes of stainless steel. *In Advanced Materials Research*, **664**(n/a), 811–16.
- Miraoui, I., Zaid, M. and Boujelbene, M. (2014). Effect of laser beam diameter on cut edge of steel plates obtained by laser machining. *Applied Mechanics and Materials*, **467**(n/a), 227–32.
- Nagarajan, R. (2000). *Parametric Study of the Effect of Laser Cutting Variables on the Cut Quality*. PhD Thesis, Wichita State University, Kansas, United States of America.
- Pandey, A. and Dubey, A. (2012). Simultaneous optimization of multiple quality characteristics in laser cutting of titanium alloy sheet. *Optics and Laser Technology*, **44**(6), 1858–65.
- Quintero, F., Pou, J., Lusquinos, F., Boutinguiza, M., Soto, R. and Perez-Amor, M. (2004). Quantitative evaluation of the quality of the cuts performed on mullite-alumina by Nd: YAG laser. *Optics and Lasers in Engineering*, **42**(3), 327–40.
- Radovanovic, M. and Madić, M. (2011). Experimental investigations of CO₂ laser cut quality: a review. *Nonconventional Technologies Review*, **15**(4), 35–42.
- Sarkar, S., Mitra, S. and Bhattacharyya, B. (2006). Parametric optimisation of wire electrical discharge machining of γ titanium aluminide alloy through an artificial neural network model. *The International Journal of Advanced Manufacturing Technology*, **27**(5), 501–08.
- Sheng, P. S. and Joshi, V. S. (1995). Analysis of heat-affected zone formation for laser cutting of stainless steel. *Journal of Materials Processing Technology*, **53**(3–4), 879–92.
- Shiue, R. K., Chang, C. T., Young, M. C. and Tsay, L. W. (2004). The effect of residual thermal stresses on the fatigue crack growth of laser-surface-annealed AISI 304 stainless steel: Part I: computer simulation. *Materials Science and Engineering*, **364**(1), 101–8.
- Topçu, İ. B., Boga A. R. and Hocaoglu F. O. (2009). Modeling corrosion currents of reinforced concrete using ANN. *Automation in Construction*, **18**(2), 145–152.
- Trochim, W. M., and Donnelly, J. P. (2001). *Research Methods Knowledge Base*. Cincinnati, OH: Atomic Dog Publishing.
- Wei, Y., Xu, Y., Dong, Z. and Zhan, X. (2009). Three-dimensional Monte Carlo simulation of discontinuous grain growth in HAZ of stainless steel during GTAW process. *Journal of Materials Processing Technology*, **209**(3), 1466–70.
- Yusoff, N., Saifu, R. I., Azuddin, M. and Aznizar, A. (2008). Selected Malaysian wood CO₂-laser cutting parameters and cut quality. *American Journal of Applied Sciences*, **5**(8), 990–6.